In Vivo Behavior of Large Doses of Ultrashort and Full-Length Single-Walled Carbon Nanotubes after Oral and Intraperitoneal Administration to Swiss Mice

Jelena Kolosnjaj-Tabi,[†] Keith B. Hartman,[‡] Sabah Boudjemaa,[§] Jeyarama S. Ananta,[‡] Georges Morgant,[†] Henri Szwarc,[†] Lon J. Wilson,[‡,*] and Fathi Moussa[†,*]

[†]UMR CNRS 8612 et Laboratoire de Bio-statistiques, Faculté de Pharmacie, Université Paris-Sud 11, 5, Rue J-B Clément Châtenay-Malabry, 92296, France, [‡]Department of Chemistry, Richard E. Smalley Center for Nanoscale Science and Technology, and Center for Biological and Environmental Nanotechnology, P.O. Box 1892, Rice University-MS 60, Houston, Texas 77251-1892, and [§]Services de Biochimie et d'Anatomie Pathologique, Groupe hospitalier Trousseau-La Roche Guyon, APHP, 22, Rue du Dr A. Netter, Paris, 75012, France

ABSTRACT Carbon nanotube (CNT) materials are of special interest as potential tools for biomedical applications. However, available toxicological data concerning single-walled carbon nanotubes (SWNTs) and multiwalled carbon nanotubes (MWNTs) remain contradictory. Here, we compared the effects of SWNTs as a function of dose, length, and surface chemistry in Swiss mice. Transmission electron microscopy (TEM), Raman, near-infrared (NIR), and X-ray photoelectron spectroscopies have been used to characterize the tested materials. The dose of SWNT materials used in this study is considerably higher than that proposed for most biomedical applications, but it was deemed necessary to administer such large doses to accurately assess the toxicological impact of the materials. In an acute toxicity test, SWNTs were administered orally at a dose level of 1000 mg/kg bodyweight (b.w.). Neither death nor growth or behavioral troubles were observed. After intraperitoneal administration, SWNTs, irrespective of their length or dose (50−1000 mg/kg b.w.), can coalesce inside the body to form fiberlike structures. When structure lengths exceeded 10 μm, they irremediably induced granuloma formation. Smaller aggregates did not induce granuloma formation, but they persisted inside cells for up to 5 months after administration. Short (<300 nm) well-individualized SWNTs can escape the reticuloendothelial system to be excreted through the kidneys and bile ducts. These findings suggest that if the potential of SWNTs for medical applications is to be realized, they should be engineered into discrete, individual "molecule-like" species.

KEYWORDS: single-walled carbon nanotubes (SWNTs) · toxicity · *in vivo* · granuloma · elimination · transmission electron microscopy (TEM)

Of the many interesting nanomaterials that are being explored in biotechnology research, carbon nanotubes (CNTs) may be the most versatile for medical applications.[1,2] However, it has been recently shown that certain formulations of multiwalled carbon nanotubes (MWNTs) can induce mesothelioma, a deadly cancer, in p53± mice following intraperitoneal (i.p.) injection[3] and in Fisher 344 rats, following intrascrotal administration.[4] Early lesions, known as granulomas, observed in mice following the i.p. administration of MWNTs are similar to those that appear on the outer lining of the lungs after the inhalation of asbestos.[3,5] These findings, considered specific for this subclass of long, unfunctionalized MWNTs, are difficult to extrapolate to other nanotube types.[6,7] Moreover, MWNTs have also been dissociated from carcinogenic potential in a very recent two-year bioassay study which used i.p. administration.[8] Fiber-length and biopersistence have been identified as the key physical properties of MWNTs that may be relevant for potential toxicity.[5] Together these considerations suggest that short and/or chemically functionalized CNTs may be preferred for future biomedical product development.[6] In this regard, ultrashort single-walled carbon nanotubes (US-tubes, less than 80 nm in length)[9] derived from full-length HiPco single-walled carbon nanotubes (SWNTs) are of special interest as potential MRI contrast,[10,11] CT contrast,[12] and radiotherapeutic agent materials.[1,13]

Available toxicological data concerning SWNTs, the form of carbon-based nanomaterials that has perhaps received the most attention for its potential applications in medicine,[1,2] are still fragmentary and subject to criticism. This is notably due to the lack of appropriate methods of characterization of nanomaterials prior to and after exposure to living cells or animals, as well as

*Address correspondence to fathi.moussa@u-psud.fr, durango@rice.edu.

Received for review November 6, 2009 and accepted January 26, 2010.

Published online February 22, 2010. 10.1021/nn901573w

TABLE 1. Characterization of the CNT Materials

	raw SWNTs[a]	purified SWNTs	US-tubes
source	Carbon Nanotechnologies, Inc.	prepared from the raw SWNTs by a non acidic treatment[28]	prepared from the raw SWNTs by fluorination and pyrolysis[9]
diameter	*ca.* 1.0 nm	*ca.* 1.0 nm	*ca.* 1.0 nm
length	>1−2 μm	*ca.* 1−2 μm	*ca.* 20−80 nm
Fe content (from ICP-OES analysis)	*ca.* 25%	*ca.* < 4%	*ca.* < 1.5%
BET surface area (m^2/g) (correlation coefficient)[b]	ND	574 (0.999056)[b]	980 (0.998694)[b]
Langmuir surface area (m^2/g) (correlation coefficient)	ND	870 (0.998647)[b]	1478 (0.999072)[b]
carbon content (atomic %, $n = 3$)[c]	ND	97.85 ± 0.05[c]	91.7 ± 0.7[c]
oxygen content (atomic %, $n = 3$)[c]	ND	2.85 ± 0.05[c]	8.3 ± 0.7[c]

[a]ND = no data. [b]Data were collected using an Autosorb-3B instruments, Quantachrome Instruments, at 77 K with nitrogen gas as adsorbate. [c]Data from X-ray photoelectron spectroscopy (XPS) analysis. The oxygen spectrum of P-SWNTs is a single peak which falls within the region for the hydroxyl group (binding energy, 531−533 eV). The oxygen spectrum of US-tubes showed two peaks with one of them in the −OH (531−533 eV) region whereas the second peak has its maximum intensity (2415 au) at 530.46 eV which is around 1.5 eV lower than that of the −OH peak. The second peak can be attributed to −COOH groups, further corroborating the increased oxygen atomic % observed for the US-tubes.

to appropriate exposure protocols.[14] Initial *in vitro* studies showed evidence of cytotoxicity induced by carbon nanotubes.[15] According to some authors the toxicity of carbon nanotubes could be due to their "surface chemistry"[16] and their degree of aggregation.[17] In contrast, other authors observed that chemical functionalization of different types of carbon nanotubes clearly reduced their cytotoxic effects.[18,19] While some reports on pulmonary[15] toxicity showed that SWNTs can also induce granuloma formation and mutagenesis,[20] other *in vivo* studies showed no sign of toxicity after intravenous (i.v.) administration of low doses (20−850 μg/kg bodyweight (b.w.)) of these nanomaterials.[21−26] Thus, the systemic toxicity as a function of dose, length, and surface chemistry of these materials remains unknown.

In this study, we have designed a protocol to investigate the acute oral toxicity as well as the acute and subchronic effects after single bolus i.p. administration of different doses of well-characterized US-tubes (containing less than 1.5% iron catalyst).[9] To address the potential effects of nanotube length, surface area, surface chemistry, and metal catalyst contamination, the effects of US-tubes were compared to those of two samples of well-characterized full-length HiPco SWNTs: raw and purified (R- and P-SWNTs, up to 2 μm in length and containing *ca.* 25% and 4% residual iron catalyst by weight, respectively).[27,28] In the following report, these three kinds of carbon nanotube materials collectively will be referred to as CNTs.

The dose of SWNT material used in this study is considerably higher than that proposed for most biomedical applications. Obviously, the exposure to such extremely high doses is unlikely to occur in the clinic or otherwise, even accidentally. Since low doses showed no acute toxicity, it was deemed necessary to administer much larger doses to accurately assess the toxicological impact of the materials.

RESULTS

CNT Characterization. Table 1 summarizes the complete characterization of the CNTs used in this study. Compared with R-SWNTs or P-SWNTs, US-tubes have a > 50% increase in surface area, presumably due to the accessibility of the US-tube interior walls. The US-tubes are 20−80 nm long and have many defects in the sidewalls, a consequence of the chemical cutting procedure.[9] The US-tube ends and sidewall defects are likely capped with carboxyl and/or hydroxyl groups, since X-ray photoelectron spectroscopy (XPS) indicated a large increase in oxygen content compared to full-length tubes. Such chemically induced defects are commonly used to functionalize SWNTs *via* an oxidation/amidation protocol.[30] Consequently, the surface interaction of US-tubes is judged to be considerably higher than that of the full-length SWNTs. Analysis by Raman spectroscopy (Figure 1) also indicated significant sp^3 character for the US-tubes compared to R-SWNTs or P-SWNTs. The ratio of the tangential mode intensity (~1590 cm^{-1}) to the disorder mode intensity (~1290 cm^{-1}) was 17.15 for the P-SWNT, but only 3.89 for the US-tubes. Additionally, there was a significant decrease in the radial breathing modes (~230 cm^{-1}) for the US-tube sample.

Aqueous suspensions of CNTs (20 mL/kg b.w. and 10 mL/kg b.w. for SWNTs) for oral administration were prepared by alternatively stirring and sonicating (in 15 min intervals, about three times daily) the mixtures in purified water for 1 month. CNTs for i.p. administration were suspended in 0.9% aqueous NaCl solution containing 0.1% Tween 60 (polyoxyethylene sorbitan monostearate, Acros Organics, Noisy-Le-Grand, France) and were stirred and sonicated for 2 months, until administrable-sized aggregates were obtained (typically less than 5 μm in diameter). As prolonged stirring/sonication could spontaneously modify the surface of CNTs (*e.g.*, hydroxylation of surface groups),[31] Raman spectroscopy was used to analyze for any possible surface modifications on the suspended tubes due to prolonged sonication and stirring. Under our conditions, Raman spectroscopy showed no evidence of surface modification.

Oral Toxicity. CNT aqueous suspensions were administered once orally at a dose level of 1000 mg/kg b.w. to mice. Neither animal death nor behavioral abnormali-

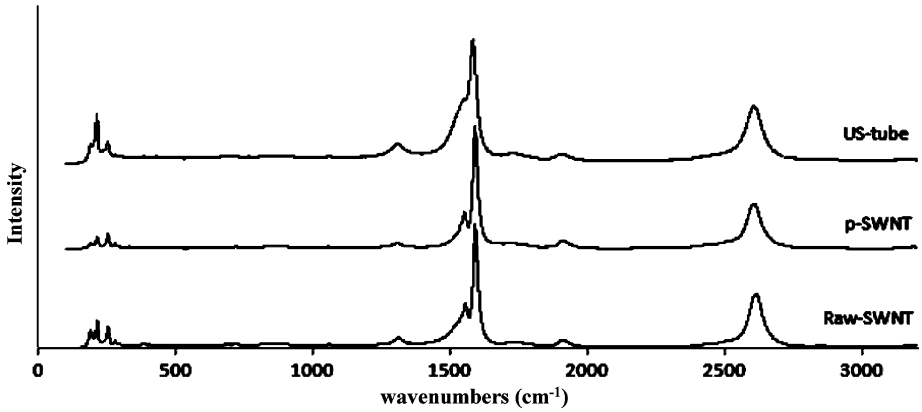

Figure 1. Raman spectrum of P-SWNTs (middle) and US-tubes (upper). The ratio of the tangential mode intensity (~1590 cm^{-1}) to the disorder mode intensity (~1290 cm^{-1}) is 17.15 for the P-SWNTs and 3.89 for the US-tubes, indicative of significantly greater sp^3 carbon character for the US-tubes. The spectrum of R-SWNTs (lower) is similar to that of P-SWNTs.

ties were observed in the control, R-SWNT, P-SWNT, or US-tube groups. Body weights of the treated animals were statistically identical to the control group (Figure 2). Compound-colored stool was found at 24 h postadministration in all treated groups. At D_{14}, irrespective of the length or of the iron content, the three CNT materials did not induce any abnormalities in the pathological examination. Thus, under these conditions, the lowest lethal dose (LD_{Lo}) is greater than 1000 mg/kg b.w. in Swiss mice.

Effects after Intraperitoneal Administration. No spontaneous animal death occurred in either experiment, confirming that the LD_{Lo} is above 1000 mg/kg b.w. in mice for US-tubes and at least above 500 mg/kg b.w. for R-SWNTs and P-SWNTs. The growth of all CNT-treated mice was identical to that of the control group (Figure 2).

Acute Effects. All mice treated with R- and P-SWNTs, irrespective of the dose, or with the lowest US-tube doses (50 and 300 mg/kg b.w.), showed no overt clinical signs or behavioral trouble. Nevertheless, the mice treated with the highest dose (1000 mg/kg b.w.) of US-tubes exhibited inactivity, lethargy, and pilo-erection until D_{14}.

Pathological Examination. After anesthesia and abdomen incision at D_{14}, several small black deposits of the injected materials were observed on most of the serosal surfaces of the organs (Figure 3). The organs of all R- and P-SWNT-treated mice, as well as those treated with the lowest dose of US-tubes (50 mg/kg b.w.), exhibited normal morphology (Figure 3b). In contrast, the organs of the animals treated with the higher US-tube doses showed different abnormalities as a function of dose. Most of the mice (4/6) treated with 300 mg/kg b.w. of US-tubes had adherent liver lobes (Figure 3c). The organs (liver, spleen, stomach, and intestine) of all animals treated with the highest dose (1000 mg/kg b.w.) were strongly adherent and covered with several large clumps of the injected material. In two cases, the deposits of the injected material were covered by a thin film of cell infiltrate (Figure 3d). In contrast to R-and P-SWNT deposits, which could be easily removed from the organ surfaces with tweezers, the clumps of US-tubes could not to be physically removed from the adherent organ surfaces.

Optical Microscopy. After hematoxylin-eosin staining, most of the organ sections of the treated animals revealed several foreign-body reactions characterized by

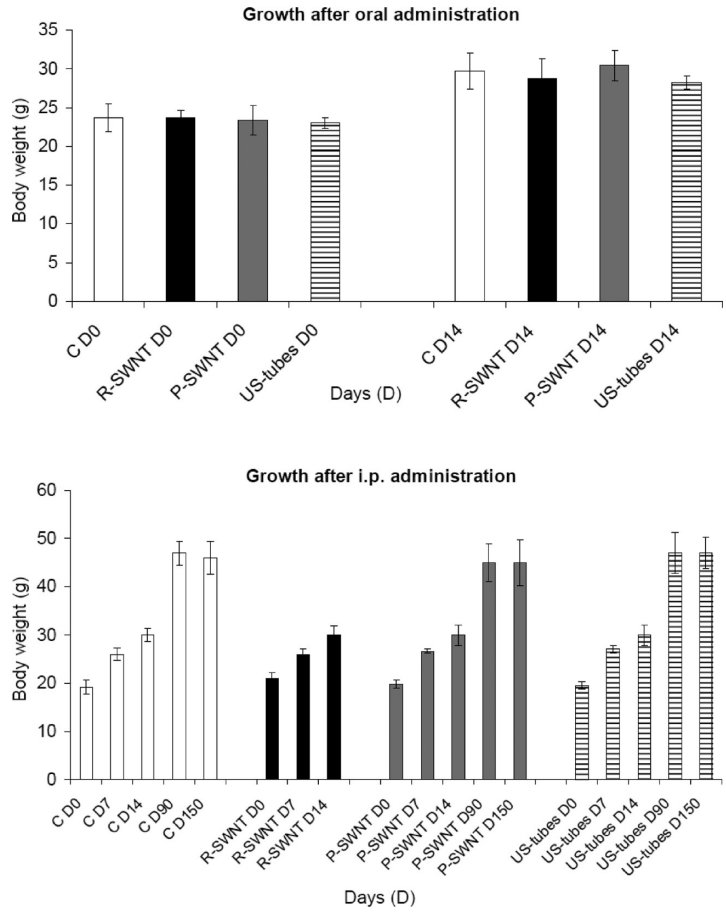

Figure 2. Animal growth (D = days). (Top) After single-dose oral administration (1000 mg/kg b.w. of nanotubes). C (control group, white bars), R-SWNT (raw SWNTs: black bars), P-SWNT (purified SWNTs, gray bars), and US-tubes (stripes). (Bottom) After single-dose intraperitoneal administration (300 mg/kg b.w. of nanotubes). The animals of the control groups (C: white) received only the vehicle. Mean and standard deviation are represented. No statistically significant changes were observed between groups.

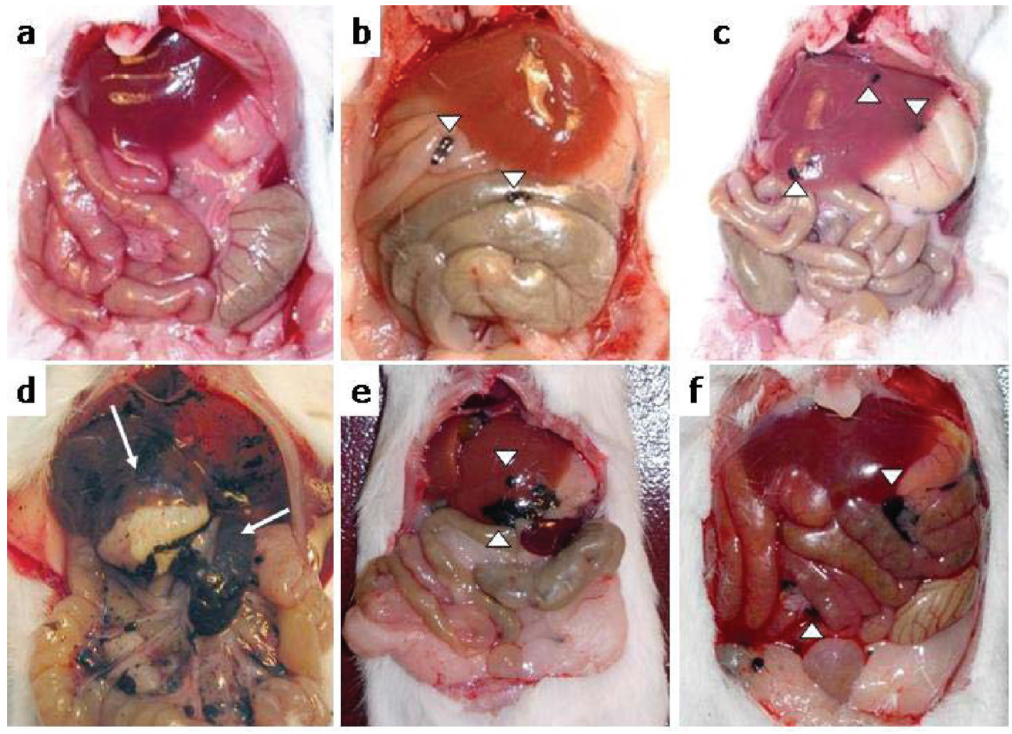

Figure 3. Peritoneal cavities of SWNT- and US-tube-treated mice, 14 and 150 days after i.p. injection. At day 14 (D14): (a) vehicle control; (b) SWNTs (50 mg/kg b.w.) with no obvious changes except black deposits (arrowheads); (c) US-tubes (300 mg/kg b.w.) inducing liver lobe adhesion; however, there were neither fibrinous deposits nor ascite retention; and (d) US-tubes (1000 mg/kg b.w.) with organ adhesion and a grayish film of cell infiltrate (arrows). At D150 (300 mg/kg b.w.): (e) SWNTs with no obvious changes except black deposits; and (f) US-tubes inducing liver lobe adhesion and slightly edematous intestinal loops.

multifocal epitheloid granulomatous lesions (Figure 4). The granulomas observed herein are similar to those already reported by others for SWNTs, both in lungs[15] and in subcutaneous tissues,[32] as well as more recently for MWNTs.[3,4,8] The severity and the localization of the granulomatous reactions were dependent on the type and the dose of the injected material.

In the animals treated with the lowest doses (50 mg/kg b.w.) of R- and P-SWNTs, only one and two out of six mice of each group, respectively, exhibited very small granulomas (less than 1 mm in diameter) exclusively located on the liver surface. In the animals treated with the highest doses (300 and 500 mg/kg b.w.), larger granulomas (2 to 5 mm in diameter) were observed on the surface of the organs. In 3 mice out of 12 treated with 500 mg/kg b.w. (1/6 and 2/6 for R- and P-SWNTs, respectively), very small granulomas were also observed inside the liver sinusoids (Figure 4a).

In the animals treated with the US-tubes, the granulomas were located both on the surface and inside the organs, irrespective of the dose. In the group treated with the lowest dose (50 mg/kg b.w.), the granulomas were very small and rare both on and inside the liver sinusoids. In the group treated with the median dose (300 mg/kg b.w.), the granulomas on the surface of the organs were more numerous and larger, while several multifocal granulomas were observed inside the livers and spleens. In this group, US-tube aggregates were frequently observed inside portal lymphatic vessels closely adjacent to hepatocytes of the limiting plate (Figure 4b). In most cases, the lymphatic vessels were connected to some large granulomas which are likely resulting from the accumulation and self-assembly of the flowing US-tube aggregates (Figure 4b,c). For the group treated with the highest dose (1000 mg/kg b.w.), a severe granulomatous reaction was observed inside the organs (Figure 4d,e). In contrast to the granulomas induced by SWNTs, which could stick out of the organ surfaces (Figure 4f), the granulomas induced by the US-tubes were strongly adherent (Figure 4g). When the granulomas were located between the liver lobes or between the organs and the surrounding tissues, they acted as "glue" leading to adherence (Figure 4d).

The increased interaction of US-tubes with organ surfaces and their strong adhesion (possibly strengthened by some intermolecular hydrogen bonding or ionic interaction) may be explained by their surface interaction. The adherence of the liver lobes, as well as the presence of confocal granulomas inside the organs in the case of US-tubes, may be explained by the rapid diffusion between the organs and inside the liver of small aggregates of US-tubes.

TEM. Although the images are not necessarily representative of the suspended CNT materials before administration to mice because of solvent evaporation and subsequent aggregation on the TEM grid, TEM micrographs show that the SWNT suspensions used in this study were mainly composed of tangled

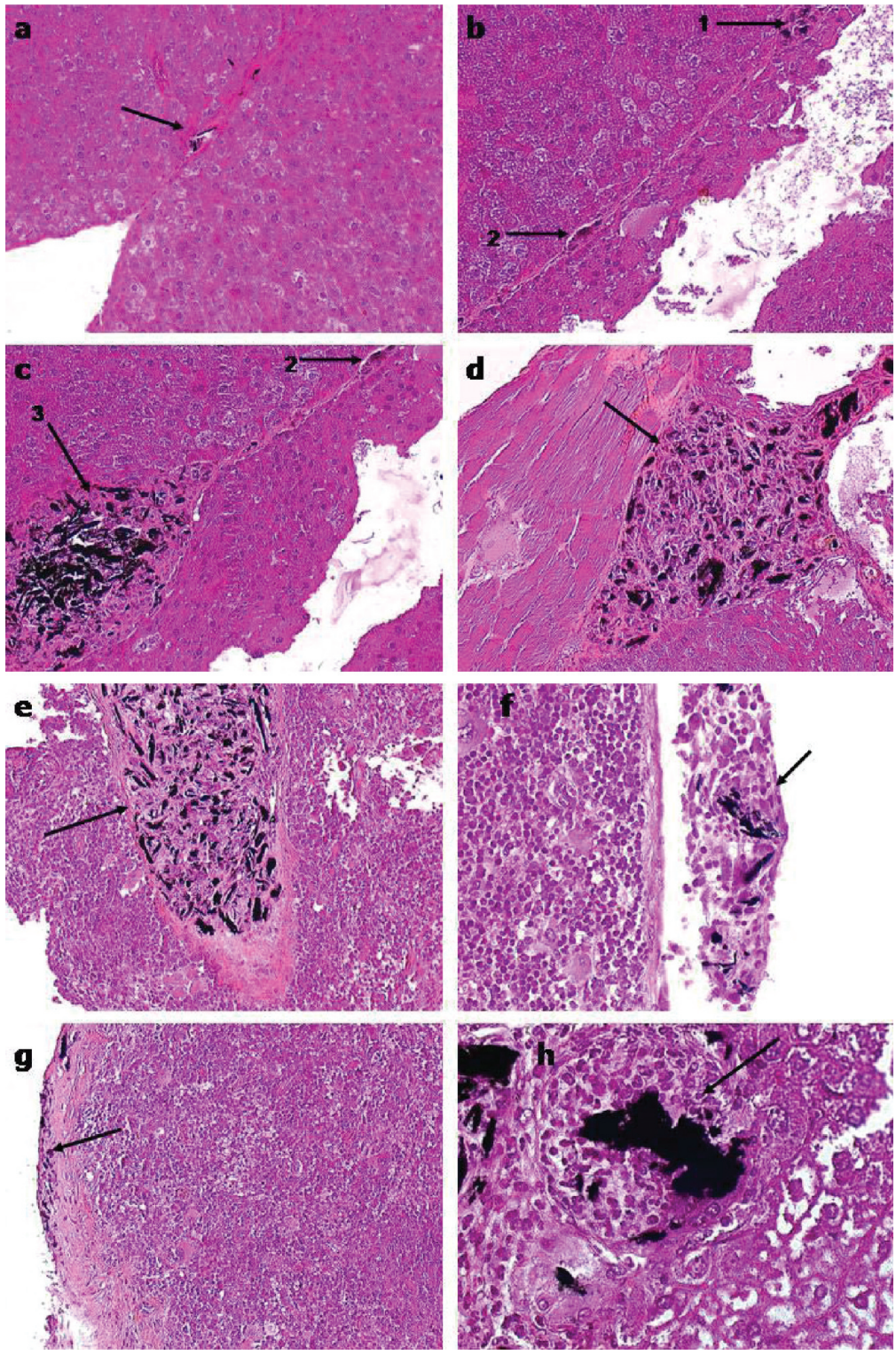

Figure 4. Light micrographs after hematoxylin-eosin staining of spleen and liver sections from mice intraperitoneally injected with a single dose of full-length SWNTs or US-tubes at 14 days postadministration. The arrows indicate (a) small SWNT aggregates inside hepatic sinusoids; (b and c) confocal granulomas and the course of US-tube aggregates inside lymphatic vessels of the liver; (d) a granuloma loaded with US-tube aggregates inducing adherence between the liver (right) and the surrounding connective tissue (left); (e) a granuloma loaded with US-tube aggregates inside the spleen; (f) a granuloma with SWNT aggregates sticking out from the spleen surface; (g) a granuloma with US-tube aggregates strongly adherent to the serosal surface of the spleen; and (h) high magnification of an US-tube-laden foreign-body-giant cell inside a granuloma. (Magnification = 40× for panels a, b, c, and f; 10× for panels d, e and g; and 100× for panel h.)

flexible bundles of nanotubes (Figure 5a,b), while the US-tube suspensions were mainly composed of short, compact bundles of aggregated US-tubes (Figure 5c). However, it is worth noting that the granu-

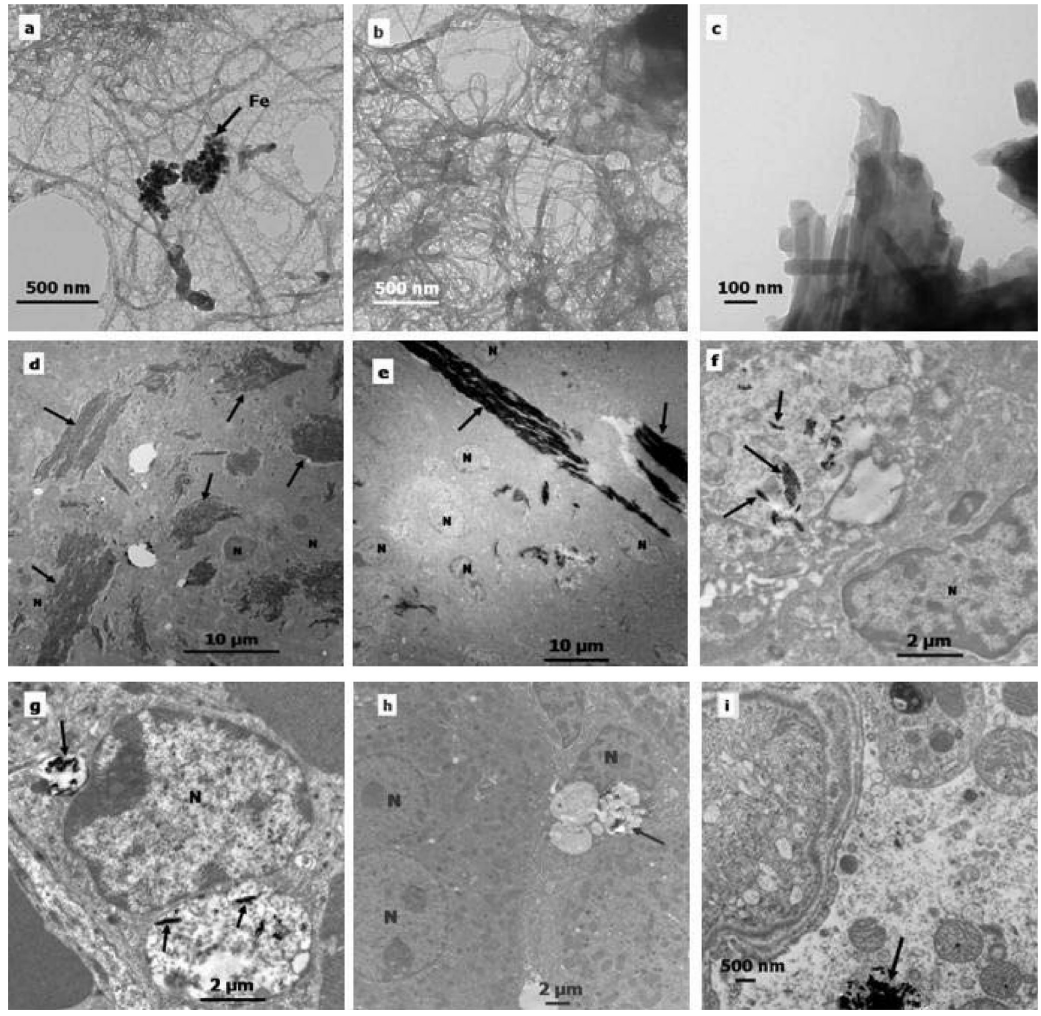

Figure 5. TEM micrographs of SWNTs and US-tubes suspended in 0.1% Tween 60, 0.9% NaCl aqueous solution: (a) R-SWNTs with large amounts of iron catalyst; (b) P-SWNTs (most of iron particles have been removed); (c) US-tubes. While the R-SWNT and P-SWNT suspensions were mainly composed of well-individualized flexible bundles of SWNTs (a, b), the US-tube suspensions were mainly composed of short, compact bundles of US-tubes that are difficult to disperse even in presence of high concentration of suspension agent (c). This is probably due to increased interactions between the US-tubes (possibly strengthened by hydrogen bonding from −OH and /or −COOH substituents). (d−i) TEM micrographs of organ sections of CNT-treated mice at D_{14}; the arrows indicate the CNT aggregates: (d) SWNT and (e) US-tube aggregates forming long fiberlike structures (mostly >10 μm) inside multimononucleate giant cells; small CNT aggregates (mostly <2 μm) without foreign-body-cell reaction inside (f) a liver macrophage, (g) a spleen macrophage, and (h) an Ito cell; (i) very small US-tube aggregates inside a renal tubule epithelial cell. (*N* = nucleus).

lomas were mainly formed by phagocytic cells and foreign-body-giant-cells (FBGCs)[33] loaded with large CNT aggregates (mostly >10 μm length). While the maximum length of US-tube bundles in the administered suspension was less than 300 nm (Figure 5c), most of the US-tube aggregates inside the granulomas are several micrometers long (>10 μm) and they exhibit fiberlike structures (Figure 5d). This is particularly true for SWNT aggregates inside the granulomas on the organ surfaces (Figure 5e). However, in contrast to short, compact bundles of US-tubes, large SWNT bundles cannot diffuse inside the organs. This explains the scarcity of granulomas inside the organs in the case of SWNTs.

The stronger aggregation of the US-tubes, as well as their increased interactions with organ surfaces may also explain why toxicological studies previously performed with CNTs, purified by a strong acidic treatment, showed harmful effects[16] since it is well-known that strong acidic treatment of R-SWNTs results in surface modification.[28,30]

In parallel with granuloma formation, numerous US-tubes and SWNT aggregates smaller than 2 μm in length were observed within phagocytic cells of liver and spleen without subsequent granulomatous reaction (Figure 5f−i). In some cases, small CNT aggregates were observed inside Ito cells like what occurs for [60]fullerene.[34,35] In very rare cases, small US-tube aggregates were observed inside renal tubule epithelium cells (Figure 5i). Microscopic examinations of all other organs (heart, lungs, and brain) did not reveal any deposit of the injected material, indicating that under these conditions most of the injected material was captured by the liver and spleen.

TABLE 2. Serum Laboratory Values 14 Days and 5 Months after Intraperitoneal Injection of Vehicle (Control), P-SWNTs, or US-Tubes[a]

	control	R-SWNTs	P-SWNTs	US-tubes
		14 Days Postadministration [SWNTs: 500 mg/kg b.w.; US-Tubes (1000 mg/kg b.w.)]		
ALT	27 (10)	48 (9) 0.03	28 (5) 0.26	70 (17) 0.02
creatinine	13.7 (2.2)	11.9 (2.7) 0.31	12.7 (2.8) 0.29	10.2 (2.4) 0.08
		5 Months Postadministration (300 mg/kg b.w.)		
glucose	6.8 (1.7)		7.6 (1.1) 0.40	5.7 (1.4) 0.30
total proteins	44 (1)		42 (2) 0.06	34 (4) 0.00
albumin	23 (2)		23 (1) 0.61	18 (3) 0.018
cholesterol	2.50 (0.29)		2.62 (0.39) 0.59	2.14 (0.63) 0.14
creatinine	15 (9)		45 (15) 0.007	17 (10) 0.69
AP	64 (14)		74 (16) 0.34	52 (12) 0.06
total bilirubin	3.6 (1.7)		4.0 (1.3) 0.69	3.2 (0.98) 0.69
ALT	30 (10)		21 (11) 0.33	19 (10) 0.15
Na	155 (2)		154 (1) 0.37	155(1) 0.85
Cl	116 (2)		117 (4) 0.45	120 (4) 0.01
vitamin A	192 (163−223)		279 (245−363) 0.003	255 (218−400) 0.05
vitamin E	1.5 (0.8−2.4)		1.8 (1.1−2.3) 0.5	1.4 (0.4−2.0) 0.85

[a]Mean values (standard deviation), or median (limits), and *p*-values as compared to the control group. Units are IU/L (alanine aminotransferase (ALT) and alkaline phosphatase (AP)), μmol/L (creatinine and total bilirubin), mmol/L (glucose, cholesterol, sodium, chloride), μg/L (vitamin A), mg/L (vitamin E), and g/L (total proteins, albumin).

Biochemical Tests. At D_{14}, circulating alanine aminotransferase activity (ALT), a classical biochemical marker of hepatholysis, of the P-SWNT-treated groups (irrespective of the dose) and of the groups treated with the lowest doses of R-SWNTs or US-tubes (<1000 mg/kg b.w.) were not significantly different from the control group (Table 2). Thus, CNTs have no acute toxic effects on liver parenchymal cells. The increase of ALT activity observed with the highest dose of R-SWNT (500 mg/kg b.w., Table 2) can be exclusively attributed to the metal catalyst. The increase of ALT activity in the case of the highest dose of US-tubes (1000 mg/kg b.w., Table 2) may be due to a vessel compression linked to the diffuse patterns of granulomas.

Elimination. After observing that some US-tube aggregates can reach the kidneys, we systematically investigated the presence of CNTs in the excreted urine and feces. TEM and high-resolution transmission electron microscopy (HRTEM) analyses of urine and feces samples from the groups treated with the highest doses of CNTs indicated the abundant presence of nanotubes, mainly SWNTs (Figure 6a). While the TEM images of urines and feces are all highly suggestive of CNT structures, they do not provide definitive proof of CNTs in the samples. To gain additional information, we have used near-infrared (NIR) fluorescence microscopy to scan urine samples from SWNT-treated mice (Figure 6g,h). NIR microscopy confirmed the presence of individualized SWNTs in the urine samples (Figure 6). SWNTs were detected in all urine samples of the mice treated with the highest doses (>300 mg/kg b.w.) until D_{14}. The maximum amount eliminated *via* the urine was observed at D_3. For US-tube samples, the extent of elimination was smaller and the period of elimination was shorter, ranging from D_1 to D_3 after administration. Although they are shorter, US-tubes were eliminated to a lesser extent than SWNTs. This is likely due to the rapid aggregation of the short, compact bundles of US-tubes and their enhanced surface interaction, which results in increased interactions with cell membranes.

When compared to the administered suspensions (Figure 5) or to the aggregated material observed inside the organs (Figure 4 and 5), the SWNTs eliminated in the urine were well-dispersed and relatively short (less than 300 nm in length) (Figure 6a). Thus, although parts of the administered aggregates were trapped inside the granulomas, a large number of short individualized SWNTs managed to reach the circulation, as confirmed by NIR microscopy. Indeed, SWNTs do not fluoresce when they are aggregated.[29] Similarly, the US-tubes eliminated in the urine correspond to the fraction of well-dispersed US-tubes present in the administered suspensions (Figure 6b). In feces, both well-dispersed individual and small compact bundles of relatively longer US-tubes were observed (Figure 6d).

Subchronic Effects. ***Pathological Examination.*** After abdomen incision at D_{150}, all treated mice (300 mg/kg b.w.) showed persistence of some black deposits. All the P-SWNT-treated mice exhibited normal organ morphology (Figure 3e). In contrast, the lobes of the livers of all the animals treated with US-tubes were adherent (Figure 3f).

Microscopy. At D_{150}, microscopic examination of organ sections of the P-SWNT-treated mice showed normal features associated with some well-circumscribed granulomas surrounded by a thin membrane, which could be easily removed from the organs (Figure 7a). In two cases out of six, relatively small, well-circumscribed granulomas were observed inside the organs (Figure 7c). In contrast, the US-tube-treated animals exhibited large and diffuse granulomas inside

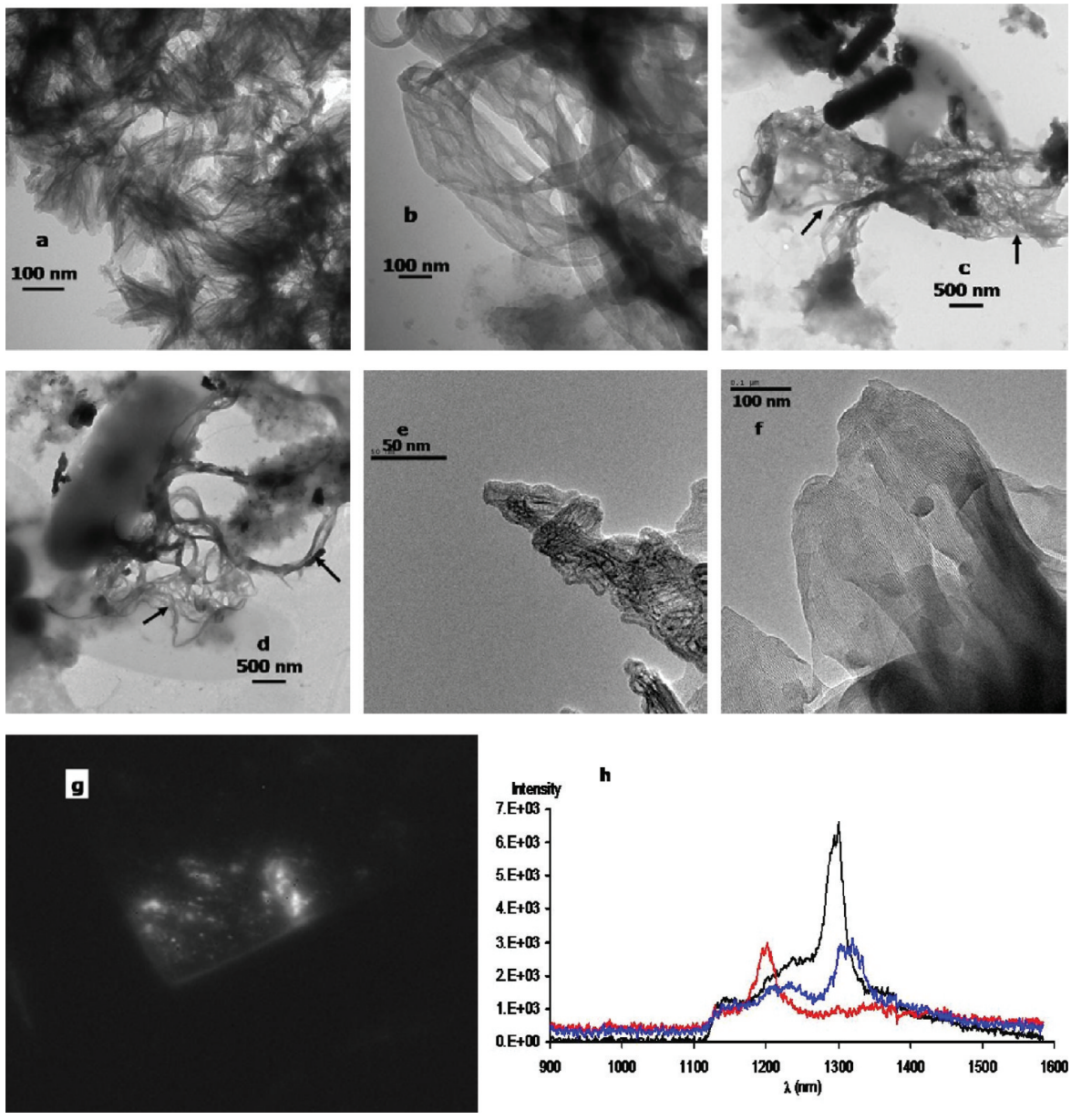

Figure 6. (a−d) TEM and (e, f) HRTEM micrographs showing CNTs in mouse urine and fecal samples 3 days postadministration. (a) Urine from P-SWNT treated mice (500 mg/kg b.w.); (b) urine and (c, d) fecal samples from the US-tube treated groups (1000 mg/kg b.w.); (e, f) HRTEM of urine samples (a, b). (g) Urine sample revealing NIR emissive spots, after 785 nm fluorescence excitation and (h) spectra of these emission features similar to that of pristine SWNTs.

both liver and spleen, tightly bound to the surrounding tissues (Figure 7b,d). Compared to D_{14}, except for a slight thickening of the membranes, the granulomas remained unchanged for both kinds of materials. The surrounding tissues remained normal without any signs of fibrosis or necrosis. In all instances, the granulomas, irrespective of their localization, only contained phagocytic cells and FBGCs, without any evidence of mesothelial lesions. However, it is highly unusual for rodents to develop mesotheliomas after such a short time period.[36]

Blood Analysis. At D_{150}, blood chemistries of the US-tube-treated group were within normal ranges and did not differ significantly from other groups, with the exception that total protein and albumin levels were slightly depressed (Table 2). At the end point, blood chemistries of the SWNT-treated group were within normal ranges, except for elevated creatinine levels which indicated a disturbance of the glomerular filtration (Table 2). This finding is particularly intriguing because microscopic examination showed neither granulomas inside the kidneys nor SWNT aggregates inside the glomerules. While small US-tube aggregates were observed inside the kidneys of the G_5 group (Figure 5i), the creatinine levels of the mice remained within normal ranges (Table 2).

In contrast to previous reports,[26] total blood counts did not differ significantly between groups at the end of the study. Normal blood counts and the absence of vitamins E and A deficiency at D_{150} showed the absence

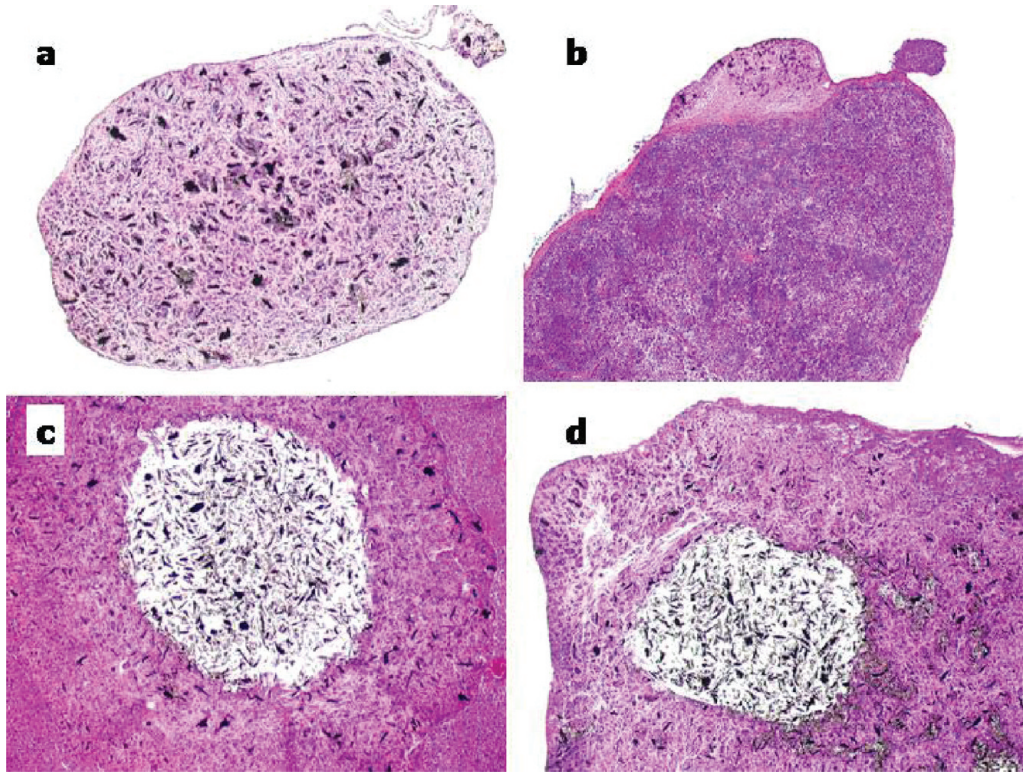

Figure 7. Light micrographs after hematoxylin-eosin staining of spleen and liver sections from treated-mice at D150 post-administration: (a) a representative granuloma sticking out from the liver surface of a SWNT-treated mouse; (b) a granuloma tightly bonded to the spleen surface of an US-tube treated mouse; (c) a well circumscribed granuloma inside a liver lobe from a SWNT-treated mouse; (d) a diffuse granuloma inside an hepatic lobe of an US-tube treated mouse. (magnification = 10×) (note the fiberlike structure of CNT aggregates).

of chronic inflammation or oxidative stress (Table 2). Vitamin E deficiency is widely used as a marker of oxidative stress,[37] while vitamin A deficiency is frequently associated with liver fibrosis.[38] However, additional studies with more animals are needed to confirm these blood-chemistry findings.

DISCUSSION

The results of the present study show, for the first time, that CNTs, irrespective of length, surface area, surface interaction, or iron content, have no acute oral toxicity after single bolus administration of up to 1000 mg/kg b.w. in mice. However, in the case of rodents, at least one route of administration should ensure full access of the unchanged substance to the circulation (European Medicines Agency, Evaluation of Medicines for Human Use, 2004). Nevertheless, a test compound should be administered to animals to identify doses causing no adverse effects and doses causing major (life-threatening) toxicity (European Medicines Agency, Evaluation of Medicines for Human Use, 2004). While initial *in vivo* studies[21−26] have shown that the i.v. injection of low doses of SWNTs (≤0.85 mg/kg b.w.) had no adverse effects, the doses causing major (life-threatening) toxicity remained unknown.

Because CNTs are insoluble in water, the i.v. administration of doses equal to or greater than 5 mg/kg b.w., which is the beginning dose for drug toxicity studies specified by the applied test guideline,[39] can lead to mechanical blockage of the vasculature system. To ensure access to the circulation for high doses of CNTs, we i.p. injected the CNTs suspended in a biocompatible medium. We anticipated that well-individualized nanotubes, as well as small aggregates present in the administered suspensions, should be cleared through lymphatics to reach the circulation *via* the thoracic duct[40] and thus target tissues. We have previously used this route to administer up to 5 g/kg b.w. of [60] fullerene (C_{60}) to mice and rats without evidence of toxicity.[34,35] Tween is widely used as a human medicine biocompatible suspension agent, and we have previously used this formulation without occurrence of toxicity.[34,35] Coating the CNTs with a dispersion agent could attenuate the difference in surface interaction between the three kinds of CNT materials used in this study. On the other hand, the dispersion agent might be rapidly displaced by blood proteins, as previously observed.[21] The dose of SWNT material used in this study is considerably higher than that proposed for most biomedical applications.[21−23] Obviously, the exposure to such extremely high doses is unlikely to occur in the clinic or otherwise, even accidentally. Besides, large bolus dosing can overwhelm clearance mechanisms. However, this approach is the only way to assess the systemic toxicity and its underlying mechanism as a function of the dose of water-insoluble materials such as pristine CNTs.

Indeed, i.p. administration of high doses of CNTs allowed a large dose of small aggregates and well-individualized nanotubes to reach the systemic circulation and subsequently tissues (and a variety of cells), through the lymphatic system, as evidenced by electron microscopy (Figure 5) and the presence of nanotubes in urine and feces (Figure 6).

Carbon nanotube toxicity is likely linked to several parameters, including catalyst contamination, particle size, surface area, surface chemistry, and interaction (also depending on the purification method), and aggregation state.[14,41] The three kinds of well-characterized CNTs(Table 1) used herein allowed us to address the effects of most of these parameters. The results obtained after i.p. administration show, for the first time, that high doses of even US-tubes can induce a granulomatous reaction because small compact bundles of US-tubes can coalesce inside the body to form large fiberlike structures. The FBGC reaction observed for US-tubes can be thus explained by the same frustrated-phagocytosis mechanism observed for long MWNTs.[3,5] This mechanism is supported by the observation that in parallel with granuloma formation, numerous US-tubes and SWNT aggregates smaller than 2 μm in length were observed within parenchymal cells of liver and spleen without subsequent granulomatous reaction (Figure 5f−i). This finding also explains why in previous studies, after i.v. administration of low doses of SWNTs, granulomatous reactions were not detected.[21,26]

Taken together, these results suggest that the key physical property of CNTs that may be relevant for potential granuloma induction is not only their length but also their ability to form fiberlike structures through aggregation. This could explain why the *in vivo* toxicity of these materials obeys the fiber-toxicity paradigm.[3,5,15,32] Large aggregates of [60]fullerene did not induce granuloma formation after i.p. administration to mice and rats,[34,35] as reconfirmed recently.[3,42] The difference in biological behavior between [60]fullerene and SWNT aggregates can be attributed to the fact that a fullerene material, a so-called "plastic crystal", is not rigid and fibrous like SWNT materials. Fullerene clusters are formed by the aggregation of lipophilic molecules, and such aggregates are basically soft and mechanically less aggressive than CNT materials.

Three main conclusions can be drawn concerning the effects of pristine CNTs after i.p. administration. The first conclusion is that, irrespective of the administered dose (50−1000 mg/kg b.w.), length, or surface interaction of the administered material, large aggregates of CNTs (>10 μm) irremediably induce granuloma formation. Even when formed by the self-assembly of US-tubes *in situ*, such aggregates exhibit fiberlike structures sufficiently large to trigger granuloma formation likely through a frustrated-phagocytosis mechanism.[5] To conclusively determine whether CNT-induced granuloma formation may result in tumor formation, we are now studying the effects of CNTs in Swiss mice for their full lifespan.

The second conclusion (as a corollary to the first) is that small aggregates of SWNTs (<10 μm) can be engulfed by phagocytes without granuloma formation. Small aggregates can be taken up by several kinds of cells with no apparent sign of toxicity. Considered together with previous findings, showing the persistence of some PEGylated-SWNTs after i.v. administration of low doses (850 μg/kg b.w.),[26] our results suggest that exposure to phagocytable-sized CNT aggregates at repeated low doses over a long period of time may lead to a granulomatous reaction through further aggregation. Thus, a toxicity study at repeated doses should be performed.

The third and final conclusion is that when CNTs are well-individualized and sufficiently short (<300 nm), they can be eliminated through the kidney and bile ducts, which has been previously observed with functionalized SWNTs[22,25] but not for the unfunctionalized SWNTs.

Finally, our studies suggest that if the potential of SWNT materials for medical applications is to be realized, they should be engineered into discrete, individual "molecule-like" species.

MATERIALS AND METHODS

Carbon Nanotube Materials: Preparation and Characterization. HiPco-produced, raw, full-length, SWNTs (R-SWNTs) were obtained from Carbon Nanotechnologies, Inc. (Houston, TX). As produced, R-SWNTs have diameters of *ca.* 1.0 nm and average lengths of *ca.* 1−2 μm, though some may be as short as several hundred nanometers or as long as 4 μm. R-SWNTs contain *ca.* 25% residual iron catalyst by weight.

Purification of R-SWNTs was achieved through a nonacidic (liquid Br_2) treatment, thus preserving the integrity of the P-SWNT sidewall and resulting in less than 4% residual iron catalyst by weight.[28] The SWNTs were chemically cut into ultrashort SWNTs (US-tubes) *via* fluorination and pyrolysis.[9] The US-tubes were then bath-sonicated in concentrated HCl for 30 min, followed by filtration and a DI water wash to remove amorphous carbon and iron catalyst impurities. US-tubes are 20−80 nm in length with less than 1.5% residual iron catalyst by weight.[9]

Raman and NIR microscopy have been performed as described previously.[9,29] Iron content of the CNT samples was determined by inductively coupled plasma optical emission spectrometry (ICP-OES) analysis. Langmuir surface area (m^2/g) of the nanotubes was determined by using an Autosorb-3B instruments (Quantachrome Instruments) at 77 K with nitrogen gas as adsorbate. Carbon and oxygen content (atomic %, $n = 3$) were determined by X-ray photoelectron spectroscopy (XPS) analysis using a PHI Quantera XPS microprobe.

Preparation of the aqueous suspensions are described in the Results Section

***In vivo* Tests.** Animals received humane care, and the study protocols complied with *Paris-Sud* University guidelines for the care and use of laboratory animals. Pathogen-free male Swiss mice (22 ± 2 g, Charles River, Arbresle, France) were housed in groups of three in individual polypropylene metabolic cages enabling urine and excrement collection at constant temperature (22 °C) and humidity (60%) and with a 12 h light/dark cycle. The mice

were fed a standard diet *ad libitum*. All mice were allowed to acclimate to this facility for at least one week before being used in the experiments.

Oral Toxicity. The oral toxicity study was conducted according to the European Community's directive.[39] After sterilization by autoclaving for 2 h at 120 °C, the resulting suspensions (1 mL/20 g b.w.) were administered orally to mice in four fractions over a period of 4 h using an intubation canula.

A total of 40 pathogen-free male Swiss mice (weighing 20 ± 2 g) were randomly divided into four groups of 10 mice each. Groups 1, 2, and 3 received the R-SWNT, P-SWNT and US-tube suspensions, respectively, and a control group received only the vehicle. The mice fasted for approximately 4 h prior to oral administration. Following the second CNT administration, the animals were provided with food and water. All animals were observed at 10 and 30 min, and 1, 2, and 4 h postdose on day 0 (D_0). The animals were then caged in metabolic cages and observed daily for 14 days, with regular monitoring of body weight.

At the end of the experiment, the animals were sacrificed for blood and organ collection after sodium pentobarbital anesthesia.

Intraperitoneal Administration. A total of 78 mice (weighing 20 ± 2 g) were randomly divided into 13 groups of six mice each (G_1 to G_{13}). Groups G_1-G_9 received an i.p. injection of a 1 mL single bolus dose of US-tubes (G_1-G_3), R-SWNTs (G_4-G_6), or P-SWNTs (G_7-G_9) at increasing doses (50, 300, and 1000 mg/kg b.w. for US-tubes and 50, 300, and 500 mg/kg b.w. for SWNTs). Groups G_{10} and G_{11} received 1 mL of the vehicle (control groups), while groups G_{12} and G_{13} received 1 mL bolus (300 mg/kg b.w.) of US-tubes and P-SWNTs, respectively. The animals were kept under observation until D_{14} for G_1-G_{10} and until D_{150} for $G_{11}-G_{13}$, under the same conditions as for the oral toxicity study.

At the end of the experiment, the animals were sacrificed for blood and organ collection after sodium pentobarbital anesthesia.

Microscopy. ***Optical Microscopy.*** Small, fresh pieces of the stomach, intestines, lungs, heart, brain, kidneys, spleen, and the right lobe of livers were fixed with pH 7.4 phosphate-buffered 10% formalin and were processed by embedding in paraffin. Organ histology was evaluated using hematoxylin and eosin or Masson's trichrome staining (Sigma-Aldrich, Steinheim, Germany).

Transmission Electron Microscopy (TEM). All the materials for the TEM; glutaraldechyde, sodium cacodylate, osmium tetraoxide, hydroxypropyl methacrylate (HMPA), Epon 812, dodecenyl succinic anhydride, methyl nadic anhydride, bensyldimethylamine (BDMA), and microscopy grids) were from EMS (Washington, DC).

Administered Suspensions. TEM samples were prepared by evaporating a drop of the CNT suspension onto a Formvar-carbon-coated (FC) copper grid. The images are not necessarily representative of the suspended CNT species before administration to mice because of solvent evaporation and subsequent aggregation on the TEM grid.

Organs. Small pieces (approximately 1 mm^3) of organs (brain, kidneys, spleen, and the right lobe of livers) were taken from the animals of each group, rinsed in physiological saline and fixed in 2% glutaraldehyde and 0.1 M sodium cacodylate buffer, pH 7.4, postfixed in 1% osmium tetroxide in buffered 0.1 M sodium cacodylate, rinsed, and dehydrated in ascending grades of ethanol and HMPA and embedded in EPON 97% (dodecenyl succinic anhydride, 22%; methyl nadic anhydride, 30%; Epon 812, 48%) and BDMA 3%. Ultrathin sections (70 nm) were cut with an Ultra-microtome. The sections were not stained prior to the observation.

Urine. A 2 mL portion of urine was mixed with 2 mL of 5 M saccharose aqueous solution. The mixture was first vortexed for 2 min and then stirred for 12 h. Afterward, the mixture was subjected to alternative sonication (15 min) and vortexing (2 min) five times. The resulting mixture was then centrifuged at 1000*g* for 10 min and the supernatant was recentrifuged at 3000*g* for 30 min. The pellet was then rinsed twice with distilled water by alternating redispersion and centrifugation at 3000*g* for 30 min. The final pellet was prepared for TEM by redispersion in 200 μL of water (sonication during 10 min). A 3 μL portion of the resulting suspension was deposed onto an ionized 400 mesh FC-coated copper grid. After 5 min, the excess of the suspension was absorbed by a slow filtration filter paper.

Feces. About 0.5 g of feces was rinsed with 2 mL of water and soaked in 3 mL of water. After adding 10 mL of a 0.1 M Tween 60 aqueous solution, the mixture was homogenized by stirring in an Ultra Turax. The final mixture was then treated twice by alternating sonication (30 min) and stirring (24 h). After decanting (30 min), the supernatant was further centrifuged at 3000*g* for 30 min. The pellet was then rinsed twice with distilled water by redispersion and centrifugation at 3000*g* (30 min). The final pellet was prepared by redispersion in 500 μL of water (sonication during 10 min). A 3 μL portion of the mixture was deposed onto an ionized 400 mesh FC-coated copper grid. After 5 min, the excess of the suspension was absorbed by a slow filtration filter paper.

NIR Microscopy. The pellets that were prepared for TEM were redispersed in 500 μL of water (sonication during 10 min). A 3 μL portion of the mixture was deposited onto an ionized 400 mesh Formvar-carbon coated copper grid. After 5 min, the excess of the suspension was absorbed by a slow filtration filter paper.

Biochemical Tests and Blood Counts. Serum biochemical tests were performed with a Hitachi 911 analyzer and complete blood counts with a XS1000i Analyzer (Roche Diagnostics, Meylan, France).

Statistics. The normality of data distribution was tested by Shapiro-Wilk test. Data are presented as the mean and standard deviation in the case of normal distributions or as the median and the range. Comparisons with control were performed by using Student test, according to the homogeneity of variances determined by Fisher test, or by Mann−Whitney test. A value of $P < 0.05$ was considered statistically significant.

Acknowledgment. The authors thank Prof. R. Bruce Weisman and Dr. Tonya Cherukuri for their help in obtaining the NIR spectra and the following for support and assistance: Robert A. Welch Foundation Grant C-0627 (L.J.W.); Nanoscale Science and Engineering Initiative of the National Science Foundation under NSF Award Number EEC-0647452 (L.J.W, K.B.H. and J.S.A); Carbon Nanotechnologies, Inc. for their generous gift of the SWNTs; Jeril Degrouard and Danielle Jaillard from the Service Commun de Microscopie Electronique (Université Paris-Sud11).

REFERENCES AND NOTES

1. Hartman, K. B.; Wilson, L. J.; Rosenblum, M. G. Detecting and Treating Cancer with Nanotechnology. *Mol. Diagn. Ther.* **2008**, *12*, 1–14.
2. Bianco, A.; Kostarelos, K.; Partidos, C. D.; Prato, M. Biomedical Applications of Functionalized Carbon Nanotubes. *Chem. Commun.* **2005**, *5*, 571–7.
3. Takagi, A.; Hirose, A.; Nishimura, T.; Fukumori, N.; Ogata, A.; Ohashi, N.; Kitajima, S.; Kanno, J. Induction of Mesothelioma in p53±Mouse by Intraperitoneal Application of Multiwall Carbon Nanotube. *J. Toxicol. Sci.* **2008**, *33*, 105–16.
4. Sakamoto, Y.; Nakae, D.; Fukumori, N.; Tayama, K.; Maekawa, A.; Imai, K.; Hirose, A.; Nishimura, T.; Ohashi, N.; Ogata, A. Induction of Mesothelioma by a Single Intrascrotal Administration of Multiwall Carbon Nanotube in Intact Male Fischer 344 Rats. *J. Toxicol. Sci.* **2009**, *34*, 65–76.
5. Poland, C. A.; Duffin, R.; Kinloch, I.; Maynard, A.; Wallace, W. A.; Seaton, A.; Stone, V.; Brown, S.; Macnee, W.; Donaldson, K. Carbon Nanotubes Introduced into the Abdominal Cavity of Mice Show Asbestos-like Pathogenicity in a Pilot Study. *Nat. Nanotechnol.* **2008**, *3*, 423–8.
6. Kane, A. B.; Hurt, R. H. The Asbestos Analogy Revisited. *Nat. Nanotechnol.* **2008**, *3*, 378–9.
7. Lacerda, L.; Ali-Boucetta, H.; Herrero, M. A.; Pastorin, G.; Bianco, A.; Prato, M.; Kostarelos, K. Tissue Histology and Physiology Following Intravenous Administration of Different Types of Functionalized Multiwalled Carbon Nanotubes. *Nanomedicine* **2008**, *3*, 149–61.
8. Muller, J.; Delos, M.; Panin, N.; Rabolli, V.; Huaux, F.; Lison, D. Absence of Carcinogenic Response to Multiwall Carbon Nanotubes in a 2-Year Bioassay in the Peritoneal Cavity of the Rat. *Toxicol. Sci.* **2009**, *110*, 442–8.
9. Gu, Z.; Peng, H.; Hauge, R. H.; Smalley, R. E.; Margrave, J. L. Cutting Single-Wall Carbon Nanotubes through Fluorination. *Nano Lett.* **2002**, *2*, 1009–13.

10. Hartman, K. B.; Laus, S.; Bolskar, R. D.; Muthupillai, R.; Helm, L.; Toth, E.; Merbach, A. E.; Wilson, L. J. Gadonanotubes as Ultrasensitive pH-Smart Probes for Magnetic Resonance Imaging. *Nano Lett.* **2008**, *8*, 415–9.
11. Sitharaman, B.; Kissell, K. R.; Hartman, K. B.; Tran, L. A.; Baikalov, A.; Rusakova, I.; Sun, Y.; Khant, H. A.; Ludtke, S. J.; Chiu, W.; *et al*. Superparamagnetic Gadonanotubes Are High Performance MRI Contrast Agents. *Chem. Commun.* **2005**, *31*, 3915–7.
12. Ashcroft, J. M.; Hartman, K. B.; Kissell, K. R.; Mackeyev, Y.; Pheasant, S.; Young, S.; van der Heide, P. A.; Mikos, A. G.; Wilson, L. J. Single-molecule I_2@US-Tube Nanocapsules: A New X-ray Contrast-Agent Design. *Adv. Mater.* **2007**, *19*, 573–6.
13. Hartman, K. B.; Hamlin, D. K.; Wilbur, D. S.; Wilson, L. J. ^{211}AtCl@US-Tube Nanocapsules: A New Concept in Radiotherapeutic Agent Design. *Small* **2007**, *3*, 1496–9.
14. Hussain, S. M.; Braydich-Stolle, L. K.; Schrand, A. M.; Murdock, R. C.; Yu, K. O.; Mattie, D. M.; Schlager, J. J.; Terrones, M. Toxicity Evaluation for Safe Use of Nanomaterials: Recent Achievements and Technical Challenges. *Adv. Mater.* **2009**, *21*, 1–11.
15. Lam, C. W.; James, J. T.; McCluskey, R.; Arepalli, S.; Hunter, R. L. A Review of Carbon Nanotube Toxicity and Assessment of Potential Occupational and Environmental Health Risks. *Crit. Rev. Toxicol.* **2006**, *36*, 189–217.
16. Magrez, A.; Kasas, S.; Salicio, V.; Pasquier, N.; Seo, J. W.; Celio, M.; Catsicas, S.; Schwaller, B.; Forró, L. Cellular Toxicity of Carbon-Based Nanomaterials. *Nano Lett.* **2006**, *6*, 1121–5.
17. Wick, P.; Manser, P.; Limbach, L. K.; Dettlaff-Weglikowska, U.; Krumeich, F.; Roth, S.; Stark, W. J.; Bruinink, A. The Degree and Kind of Agglomeration Affect Carbon Nanotube Cytotoxicity. *Toxicol. Lett.* **2007**, *168*, 121–31.
18. Sayes, C. M.; Liang, F.; Hudson, J. L.; Mendez, J.; Guo, W.; Beach, J. M.; Moore, V. C.; Doyle, C. D.; West, J. L.; Billups, W. E.; *et al*. Functionalization Density Dependence of Single-Walled Carbon Nanotubes Cytotoxicity *in Vitro*. *Toxicol. Lett.* **2006**, *161*, 135–42.
19. Dumortier, H.; Lacotte, S.; Pastorin, G.; Marega, R.; Wu, W.; Bonifazi, D.; Briand, J. P.; Prato, M.; Muller, S.; Bianco, A. Functionalized Carbon Nanotubes are Noncytotoxic and Preserve the Functionality of Primary Immune Cells. *Nano Lett.* **2006**, *6*, 1522–8.
20. Shvedova, A. A.; Kisin, E.; Murray, A. R.; Johnson, V. J.; Gorelik, O.; Arepalli, S.; Hubbs, A. F.; Mercer, R. R.; Keohavong, P.; Sussman, N.; *et al*. Inhalation *vs*. Aspiration of Single-Walled Carbon Nanotubes in C57BL/6 Mice: Inflammation, Fibrosis, Oxidative Stress, and Mutagenesis. *Am. J. Physiol. Lung Cell Mol. Physiol.* **2008**, *295*, 552–65.
21. Cherukuri, P.; Gannon, C. J.; Leeuw, T. K.; Schmidt, H. K.; Smalley, R. E.; Curley, S. A.; Weisman, R. B. Mammalian Pharmacokinetics of Carbon Nanotubes Using Intrinsic Near-Infrared Fluorescence. *Proc. Natl. Acad. Sci. U.S.A.* **2006**, *103*, 18882–6.
22. Singh, R.; Pantarotto, D.; Lacerda, L.; Pastorin, G.; Klumpp, C.; Prato, M.; Bianco, A.; Kostarelos, K. Tissue Biodistribution and Blood Clearance Rates of Intravenously Administered Carbon Nanotube Radiotracers. *Proc. Natl. Acad. Sci. U.S.A.* **2006**, *103*, 3357–62.
23. Yang, S. T.; Guo, W.; Lin, Y.; Deng, X. Y.; Wang, H. F.; Sun, H. F.; Liu, Y. F.; Wang, X.; Wang, W.; Chen, M.; *et al*. Biodistribution of Pristine Single-Walled Carbon Nanotubes *in Vivo*. *J. Phys. Chem. C* **2007**, *11*, 17761–4.
24. Liu, Z.; Cai, W.; He, L.; Nakayama, N.; Chen, K.; Sun, X.; Chen, X.; Dai, H. *In Vivo* Biodistribution and Highly Efficient Tumor Targeting of Carbon Nanotubes in Mice. *Nat. Nanotechnol.* **2007**, *2*, 47–52.
25. Liu, Z.; Davis, C.; Cai, W.; He, L.; Chen, X.; Dai, H. Circulation and Long-Term Fate of Functionalized, Biocompatible Single-Walled Carbon Nanotubes in Mice Probed by Raman Spectroscopy. *Proc. Natl. Acad. Sci.* **2008**, *105*, 1410–5.
26. Schipper, M. L.; Nakayama-Ratchford, N.; Davis, C. R.; Kam, N. W.; Chu, P.; Liu, Z.; Sun, X.; Dai, H.; Gambhir, S. S. A Pilot Toxicology Study of Single-Walled Carbon Nanotubes in a Small Sample of Mice. *Nat. Nanotechnol.* **2008**, *3*, 216–21.
27. Nikolaev, P.; Bronikowski, M. J.; Bradley, R. K.; Rohmund, F.; Colbert, D. T.; Smith, K. A.; Smalley, R. E. Gas-Phase Catalytic Growth of Single-Walled Carbon Nanotubes from Carbon Monoxide. *Chem. Phys. Lett.* **1999**, *313*, 91–7.
28. Mackeyev, Y.; Bachilo, S.; Hartman, K. B.; Wilson, L. J. The Purification of HiPco SWCNTs with Liquid Bromine at Room Temperature. *Carbon* **2007**, *45*, 1013–7.
29. Tsyboulski, D. A.; Bachilo, S. M.; Weisman, R. B. Versatile Visualization of Individual Single-Walled Carbon Nanotubes with Near-Infrared Fluorescence Microscopy. *Nano Lett.* **2005**, *5*, 975–9.
30. Tasis, D.; Tagmatarchis, N.; Bianco, A.; Prato, M. Chemistry of Carbon Nanotubes. *Chem. Rev.* **2006**, *106*, 1105–36.
31. Moonoosawmy, K. R.; Kruse, P. To Dope or Not To Dope: The Effect of Sonicating Single-Wall Carbon Nanotubes in Common Laboratory Solvents on Their Electronic Structure. *J. Am. Chem. Soc.* **2008**, *130*, 13417–24.
32. Koyama, S.; Endo, M.; Kim, Y. A.; Hayashi, T.; Yanagisawa, T.; Osaka, K.; Koyama, H.; Haniu, H.; Kuroiwa, N. Role of Systemic T-Cells and Histopathological Aspects after Subcutaneous Implantation of Various Carbon Nanotubes in Mice. *Carbon* **2006**, *44*, 1079–92.
33. Anderson, J. M.; Rodriguez, A.; Chang, D. T. Foreign Body Reaction to Biomaterials. *Semin. Immunol.* **2008**, *20*, 86–100.
34. Moussa, F.; Trivin, F.; Ceolin, M.; Hadchousel, P. Y.; Sizaret, V.; Greugny, V.; Fabre, C.; Rassat, A.; Szwarc, H. Early Effects of C60 Administration in Swiss Mice: A Preliminary Account for *in Vivo* C60 Toxicity. *Fullerene Sci. Technol.* **1996**, *4*, 21–9.
35. Gharbi, N.; Pressac, M.; Hadchouel, M.; Szwarc, H.; Wilson, S. R.; Moussa, F. [60]Fullerene is a Powerful Antioxidant *in Vivo* With No Acute or Subacute Toxicity. *Nano Lett.* **2005**, *5*, 2578–85.
36. Marsella, J. M.; Liu, B. L.; Vaslet, C. A.; Kane, A. B. Susceptibility of p53-Deficient Mice to Induction of Mesothelioma by Crocidolite Asbestos Fibers. *Environ. Health. Perspect.* **1997**, *105*, 1069–72.
37. Poli, G. Pathogenesis of Liver Fibrosis: Role of Oxidative Stress. *Mol. Aspects. Med.* **2000**, *21*, 49–98.
38. Geerts, A.; De Bleser, P.; Hautekecte, M. L.; Nild, T.; Wisse, E.; Fat-Storing (Ito) Cell Biology. In *The Liver: Biology and Pathobiology*, 3rd ed.; Arias, I. M.; Boyer, J. L.; Fausto, N.; Jakoby, W. B.; Schater, D. A.; Shafritz, D. A.; Eds.; Raven Press Ltd: New York, 1994; pp 819−839.
39. EC Commission Directive 2004/73/EC of 29 April 2004 Adapting to Technical Progress for the Twenty-Ninth Time Council Directive 67/548/EEC on the Approximation of the Laws, Regulations and Administrative Provisions Relating to the Classification, Packaging and Labeling of Dangerous Substances. O.J. No. L1522004.
40. Courtice, F. C. The Origin of Lipoprotein in Lymph. In *Lymph and the Lymphatic System*; Meyersen, H. S., Ed.; C.C. Thomas: New York, 1963, pp 89−126.
41. Donaldson, K.; Aitken, R.; Tran, L.; Stone, V.; Duffin, R.; Forrest, G.; Alexander, A. Carbon Nanotubes: A Review of Their Properties in Relation to Pulmonary Toxicology and Workplace Safety. *Toxicol. Sci.* **2006**, *92*, 5–22.
42. Mori, T.; Takada, H.; Ito, S.; Matsubayashi, K.; Miwa, N.; Sawaguchi, T. Preclinical Studies on Safety of Fullerene upon Acute Oral Administration and Evaluation for No Mutagenesis. *Toxicology* **2006**, *225*, 48–54.